

STRESS CONCENTRATIONS IN SCREW THREADS

G. Peter O'Hara
US Army Armament Research and Development Command
Benet Weapons Laboratory, LCWSL
Watervliet Arsenal, Watervliet, NY 12189

SUMMARY

The concept of stress concentration in screw threads is defined as a ratio of maximum fillet stress normalized to shear transfer rate. The data is presented as a plot of fillet stress vs. radial stress for a particular thread form. The Heywood equation is used to generate the basic plots and NASTRAN is used to extend the analysis to the case both where flanks of an individual thread tooth are in contact and the case where a finite axial stress is superimposed.

INTRODUCTION

The concept that stress or flow lines concentrate around various structural discontinuities is very old and has been the subject of many thousands of books and technical papers. It is convenient to express this concept in terms of a stress concentration factor (K) using the simple equation:

$$\sigma_{\max} = K \sigma_{\text{non}}$$

Where K is a ratio between the maximum stress and some nominal stress, the single book "Stress Concentration Factors" by R. E. Peterson (ref. 1) is a compilation of the work included in some 378 references. The bulk of this work is contained on graphs which are plots of K vs. some geometry factor and most use a family of curves to show the effect of some other geometry factor. These plots provide both useful numeric information and a quick visual picture of the structural response.

The concept of stress concentration in screw threads is rather elusive and in fact there is little work done on stresses in threads. R. B. Heywood (ref. 2) published an empirical equation for the maximum fillet stress which was used in the work of Weigle, Lasselle and Purtell (ref. 3) as a guide in trying to improve fatigue life of cannon breech rings. Later this author demonstrated that the Heywood equation would give accurate numeric data when the boundary conditions were closely controlled (ref. 4).

However, most work with screw threads seems to be done for specific cases such as the fine work of M. Heyinyi (ref. 5) who investigated bolt shank and nut design in Witworth threaded bolts. This type of analysis using three dimensional photoelasticity was also used by W. F. Franz (ref. 6) and J. D. Chalupnik (ref. 7). A further attempt at optimizing a thread form was done by

R. L. Marino and W. F. Riley (ref. 8).

In all of these works the calculated stress concentration factor is different for each thread in the system. It would seem that if the stress concentration factor is properly defined something should be a constant for all threads of a specific shape. In his original paper, Heywood demonstrated part of the problem. The stress in the fillet is the result of two factors. First, is the stress due to the load on the individual thread tooth and second, is the stress due to the general stress field or the axial stress (σ_a) near the thread fillet. In this paper I will add effect due to friction and normalize all stresses to the average shear transfer rate (τ_R).

When the friction force and the force due to the "wedge" effect of the loaded flank of the thread are combined a radial (normal) force is produced which can be averaged into the radial stress (σ_r). The fillet stress (σ_F) can be expressed as the sum of two functions.

$$\sigma_F/\tau_R = \bar{\sigma}_F = G_1(\alpha, \beta, \bar{R}, \theta, \bar{\sigma}_r) + G_2(\alpha, \beta, \bar{R}, \theta, \bar{\sigma}_a)$$

In the above equation the first function (G_1) is the relation between fillet stress and the load on the individual thread tooth. The second function (G_2) is the factor due to the general stress field. Alpha (α), beta (β) and \bar{R} are the thread geometry factors. The angle (θ) is in both functions because they do not maximize at the same position in the fillet. In this paper the shear transfer rate is defined as the net load supported by the thread divided by the area at the pitch line. The direction of the net load is parallel to the pitch line and in the analysis this component of the force will be unity. The radial stress ($\bar{\sigma}_r$) and axial stress ($\bar{\sigma}_a$) are normalized to the shear transfer rate.

The above discussion relates to a normal screw thread problem where only one flank of a particular thread contacts one flank of a mating thread. In some structures the relative displacement in the radial direction across the threaded connection is such that the radial gap in the threads is closed and both flanks of each thread carry load. Under these conditions the radial component of the loads add together to produce high negative or compressive radial stress across the joint. The axial loads oppose each other and the pressure on the primary flank must become very high to overcome the secondary flank load. This is not a common condition; however, it may become very important in the cannon breech-to-tube connection.

THREAD GEOMETRY

The thread geometry parameters are shown in Figure 1 and in this report all linear dimensions will be normalized to pitch (P). The primary geometry parameters are the primary flank angle (α), the secondary flank (β) and the root radius \bar{R} . These, in conjunction with the pitch space (P_1), define the basic thread geometry. Other factors are required to insure a practical thread which will fit together. The addendum (AD) and dedendum (DD) dimensions sum to the

total height (HT). The tip radius (RT) eliminates a sharp corner and helps to support the bearing surface. The root flat (FLAT) is often used to make up for the root radius tolerance. The bearing height (Z) is used to calculate the average bearing stress and the shear length (S) is used to calculate the maximum shear-out failure load.

This complicated system is simplified by the fact that we must deal with a small set of standard thread forms. In this report detailed analysis has been done on the British Standard Buttress thread and Heywood analysis has also been done on the controlled root bolt thread or "J" thread and the Watervliet Arsenal Buttress used on cannon breeches. The nominal dimensions for these threads are shown in Table I.

TABLE I. THREAD GEOMETRY DEFINITION

	British Buttress	Watervliet Buttress	30 "V" (Rolled)
α	7°	20°	30°
β	45°	45°	30°
\bar{R}	0.1205	0.1333	0.1804
P1	0.500	0.5276	0.500
HT	0.5059	0.4787	0.6077
RT	0.00	0.0480	0.1083
FLAT	0.0	0.0	0.0

LOADING PARAMETERS

The Heywood load parameters are also shown in Figure 1. They are a point force (W) applied at some position (b) in the loaded flank with a friction angle (γ). This scheme can be repeated many times on the loaded flank to produce some load distribution curve. The following loading assumptions are made:

1. The total load vector parallel to the datum line is unity.
2. The load distribution is uniform.
3. Friction does not vary along the flank.

The first assumption given allows the normalization of stresses to shear transfer rate and the other two establish a simple loading case.

Under conditions of high radial compressive load, it is possible for threads to be pushed together until both flanks contact. This condition will be discussed later. Under normal conditions only the primary flanks contact on the thread and the radial stress become a function of the flank angle α and the friction angle γ :

$$\bar{\sigma}_r = \tan (\alpha-\gamma)$$

Note that friction becomes a signed variable depending on the relative displacement of the two components of the structure.

In the above discussion the general field or axial stress is assumed to be zero. In the NASTRAN finite element analysis the axial stress was simulated by the use of a constraint subcase in which the relative axial displacement between the two radial boundaries was fixed by the use of scalar points and multipoint constraint equations. The radial displacements on these planes were made equal for congruent points. The radial displacement of the inner axial boundary was set equal to the Poisson contraction of a solid bar.

HEYWOOD ANALYSIS

The Heywood equation is shown in Figure 2. This is a semi-empirical equation that was fit to a large body of photoelastic data. It calculates maximum fillet stress for a point load on the primary flank of a thread using a specific friction angle. In order to simulate a uniform load distribution, the results are averaged for seven different "b" values evenly distributed over the flank. The process has been programmed into a program called HEY40. The calculations have been done for many standard thread forms, and the three reported in Figure 3, have been defined in Table I. This plot of fillet stresses plotted against radial stress will be referred to as the "thread characteristic curve". This curve covers a friction angle range of -45° to 45° or a coefficient of friction range of -1.0 to 1.0.

In Heywood's photoelastic experiments he was careful to transfer the load supported by the threads profiles in a shear mode to make the axial stress as small as possible. This process limited his equation to the case where axial stress is equal to zero.

NASTRAN FINITE ELEMENT ANALYSIS

The finite element work was done for three reasons: (1) to verify the Heywood analysis; (2) to examine the two-flank problem; and (3) to include a finite axial stress. The grid for the British Standard Buttress is shown in Figure 4. It contains 216 triangular ring elements (CTRIARG) and 133 grid points. The run required five basic loading subcases plus fourteen subcase combinations for each value of axial stress. These fourteen subcases cover both 1-flank and 2-flank contact over a range coefficient of friction of -1.0 to 1.0 in increments of 0.25.

The grid was generated using IGFES (ref. 9) and following that, force sets were calculated to apply uniform pressure and uniform shear loads on both flanks of the thread and a displacement was calculated for a nominal 1.0 psi axial load on the grid. Two different constraint conditions were required to complete the boundary conditions for a single thread taken from a long series of threads. For loads on the thread the inner boundary points were fixed in both radial and

axial directions and similar points on the two radial boundaries were constrained to equal displacements. In this way the net load was taken out as shear load on the inner axial boundary and the multipoint constraint equations replaced adjoining material. For the axial load condition the inner axial boundary was constrained to the Poisson displacement in the radial direction and left free in the axial direction. The two radial boundaries were given fixed relative axial displacements and the radial displacement was made equal for similar grid points. This condition was set to simulate a far removed axial loading.

Because the basic loads were all for a 1.0 psi uniform applied pressure or shear and the results were desired for a 1.0 psi shear transfer rate (calculated at the datum line), it became necessary to calculate the correct Subcase Sequence Coefficients for fourteen subcases for each of four axial stress values (or 56 sets). Therefore a small program was generated to supply all necessary SUBCOM, SUBSEQ and LABEL cards for that portion of the case control deck.

Uniform increments of 0.25 in coefficient were used from -1.0 to 1.0. If the friction value was positive, a single subcase combination was generated which would superimpose the two primary flank loads with the proper value of axial stress. If the friction was zero or less, a similar subcase combination was generated along with one where both flanks were loaded and the second radial stress was 1.0 greater than the initial.

The axial load subcase produced the conventional fillet stress concentration factors of $K = 2.89$. This maximum stress was in an element at the bottom of the fillet where θ is approaching 0° . In the cases where the load is applied to the thread the exact position of the stress maximum is about 45° up from the bottom of the fillet. Data is reported here for two cases of axial stress. Zero axial stress is shown in Figure 5 and axial stress of 2.0 is shown in Figure 6. These plots are a set of six lines with the single contact curve at the right. Starting at that curve is a family of five lines going to the left which represent two flank contacts at different values of friction from 0 to -1.0.

DISCUSSION

The first thing to note is that there is excellent agreement between Heywood and NASTRAN over most of the range of the plots for the one case in question. Because of this, the Heywood relation can be used to evaluate different thread forms. The finite element method has allowed the expansion of the basic plot to the 2-flank contact problem and the addition of the axial stress.

There are several important points that are demonstrated by this work. Note that a small change in friction can produce a large fillet stress variation in all three threads reported in the Heywood analysis. Negative friction angles can produce marked reductions in thread fillet stress. This effect was noted several years ago in an unpublished three dimensional photoelastic study where the model was overloaded and the threads were forced to a high negative radial

stress. In this case the fillet stresses were very low and the experiment was repeated. This author suspects that friction variation may be responsible for much of the scatter in bolt-fatigue data.

This work was initiated because of the necessity of analyzing a structure with a long threaded connection using many small threads. In this case the modeling of each thread would require an excessively large data deck. Therefore, the threads were handled as a conventional contact problem where friction could take on any value and limits were applied to the radial stress. In the solution the contact surface was placed on the datum line of the threads and one or two teeth were replaced by one element space. Shear transfer rates could then be estimated from the shear stress data near the contact surface along with radial and axial stress. The fillet stresses were estimated for use in fracture mechanics analysis.

CONCLUSION

A stress concentration approach to the thread fillet stress problem has been defined using the shear transfer rate as the fundamental quantity. This stress concentration is plotted for a fixed geometry in a stress vs. stress plot where the stress concentration is a function of the applied radial stress. This process can be repeated for several values of the applied axial load. The effects of axial stress and applied thread loads seem to be of equal importance and accurate results require the analysis of both factors.

REFERENCES

1. "Stress Concentration Factors," R. E. Peterson, John Wiley & Sons, New York, 1974.
2. Heywood, R. B., "Tensile Fillet Stresses in Loaded Projections," Proceedings of the Institute of Mechanical Engineers, Vol. 160, p. 124, 1960.
3. Weigle, Lasselle and Purtell, "Experimental Behavior of Thread-Type Projections," Experimental Mechanics, May 1963.
4. O'Hara, G. P., "Finite Element Analysis of Threaded Connections," Proceedings of the Fourth Army Symposium on Solid Mechanics, September 1974.
5. Hetinyi, M., "The Distribution of Stress in Threaded Connections," Proceedings of SESA, Vol. 1, No. 1, 1943.
6. Franz, W. F., "Three-Dimensional Photoelastic Stress Analysis of a Threaded Pipe Joint," Proceedings of SESA, Vol. , No. , 1950.
7. Chalupnik, J. D., "Stress Concentration in Bolt Thread Roots," Experimental Mechanics, 1967.

8. Marino, R. L., and Riley, W. F., "Optimizing Thread-Root Contours Using Photoelastic Methods," *Experimental Mechanics*, January 1964, p. 1.
9. Lorensen, W. E., "Interactive Graphic Support for NASTRAN," *Sixth NASTRAN User's Colloquium*, NASA Conference Publication 2018, October 1977.

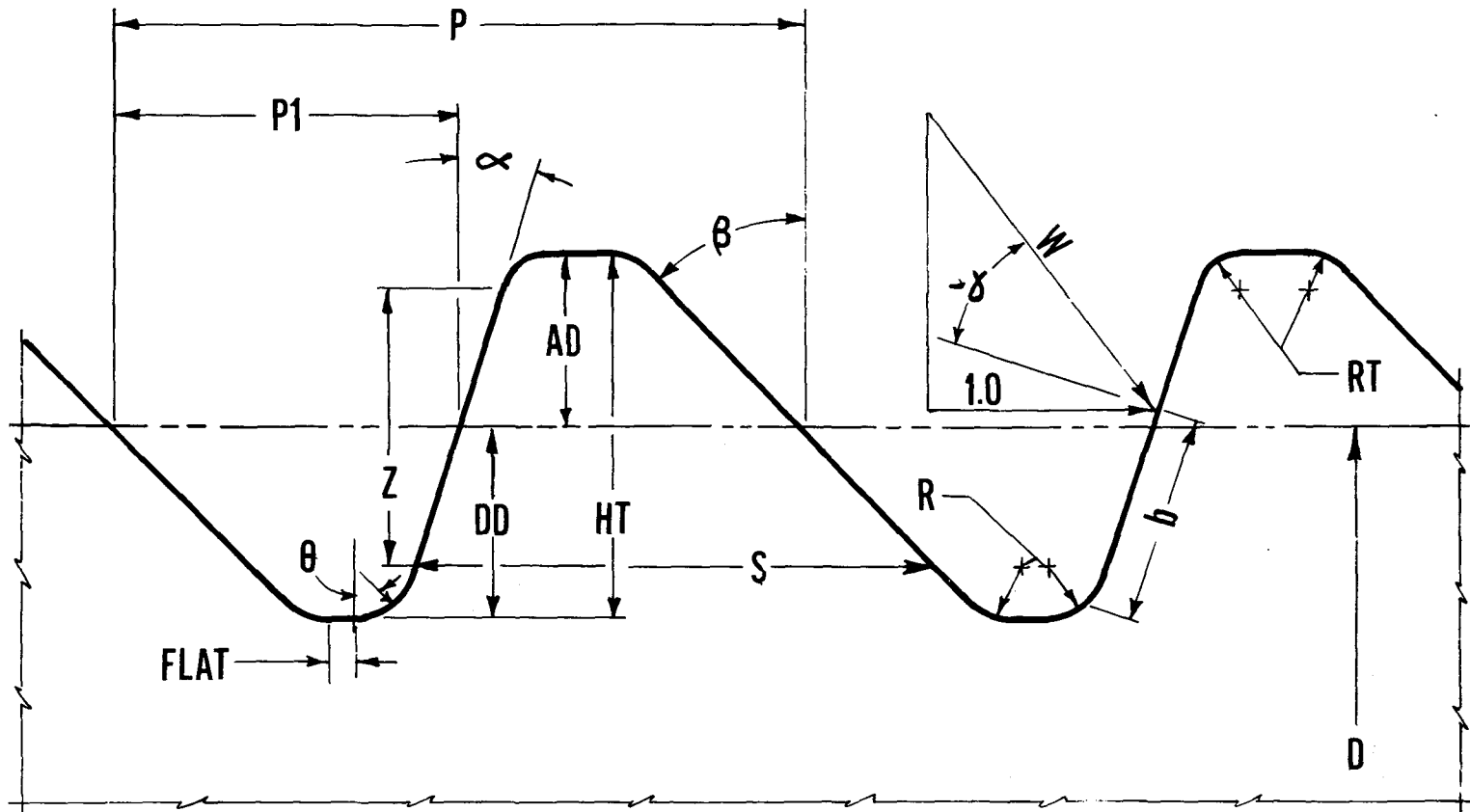


Figure 1. THREAD GEOMETRY AND LOAD PARAMETERS

$$\sigma_F = \left[1.0 + 0.26 \left(\frac{e}{R} \right)^{0.7} \right] \left[\frac{1.5}{e^2} + \sqrt{\frac{0.36}{be}} \left(1.0 + \frac{1}{4} \sin \delta \right) \right] \frac{W}{T}$$

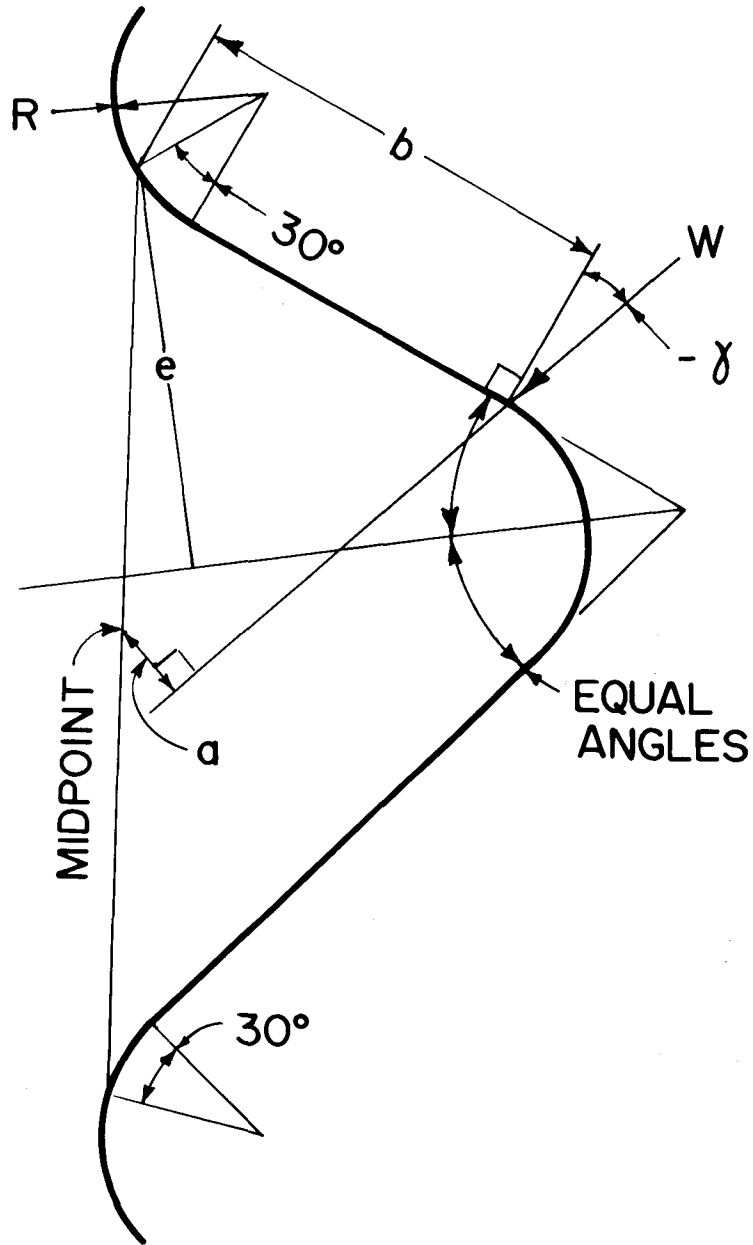


Figure 2. HEYWOOD'S EQUATION

**THREAD CHARACTERISTIC FROM
HEYWOOD ANALYSIS FOR:**

① = **BRITISH STANDARD BUTTRESS**

② = **WATERVLIET BUTTRESS**

③ = **CONTROLLED ROOT "V"**

$$\bar{\sigma}_a = 0.0$$

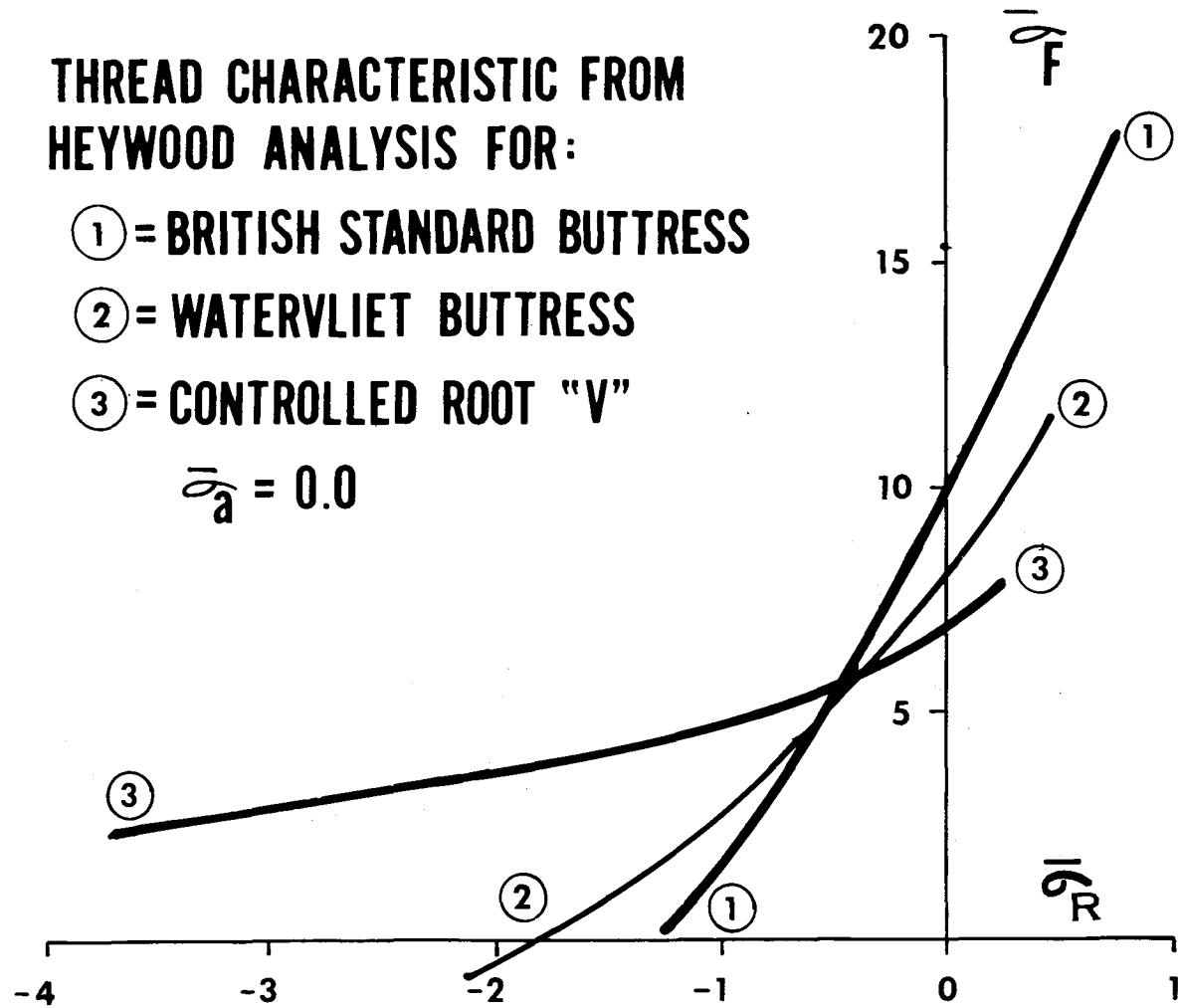


Figure 3.

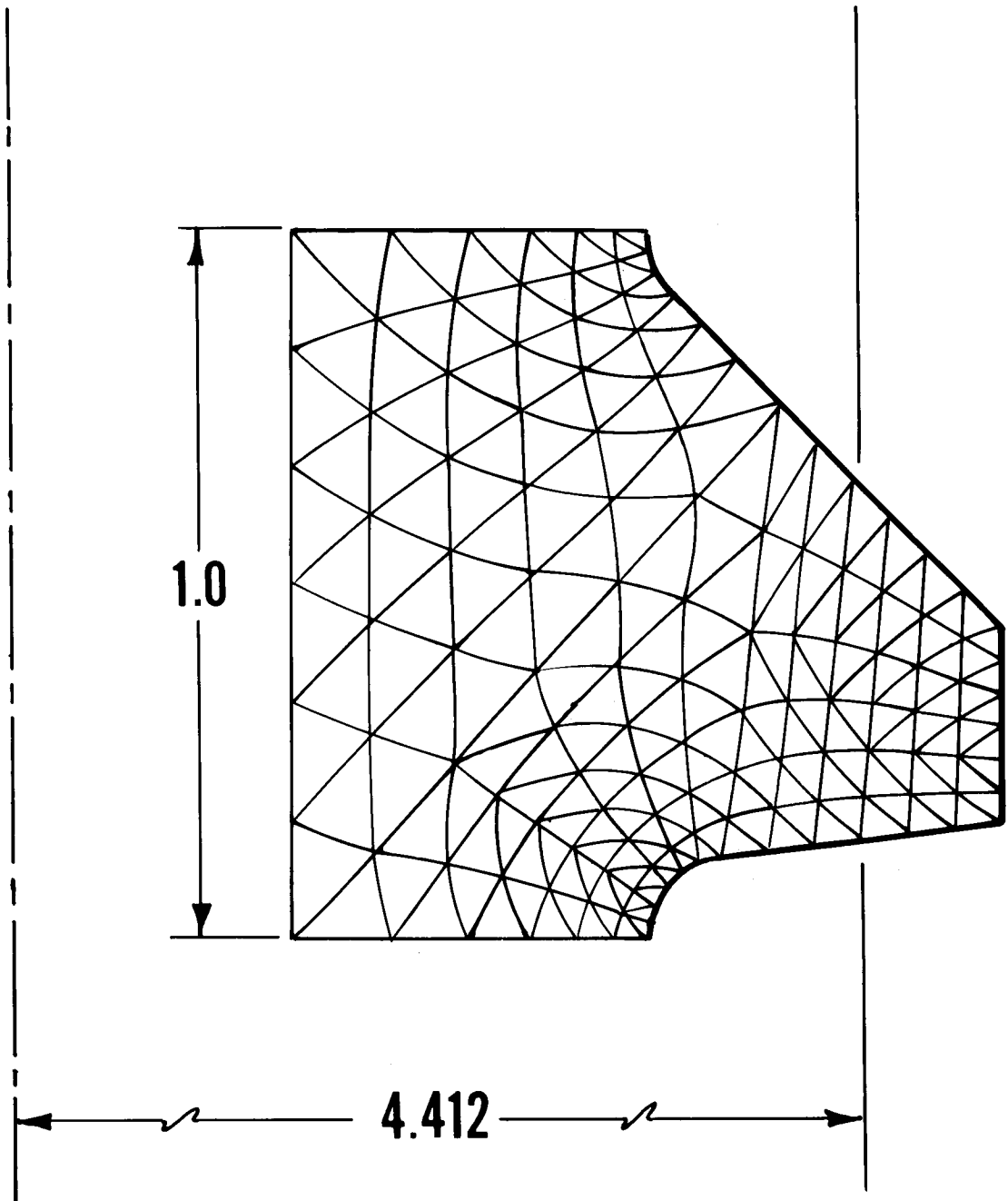


Figure 4. NASTRAN GRID

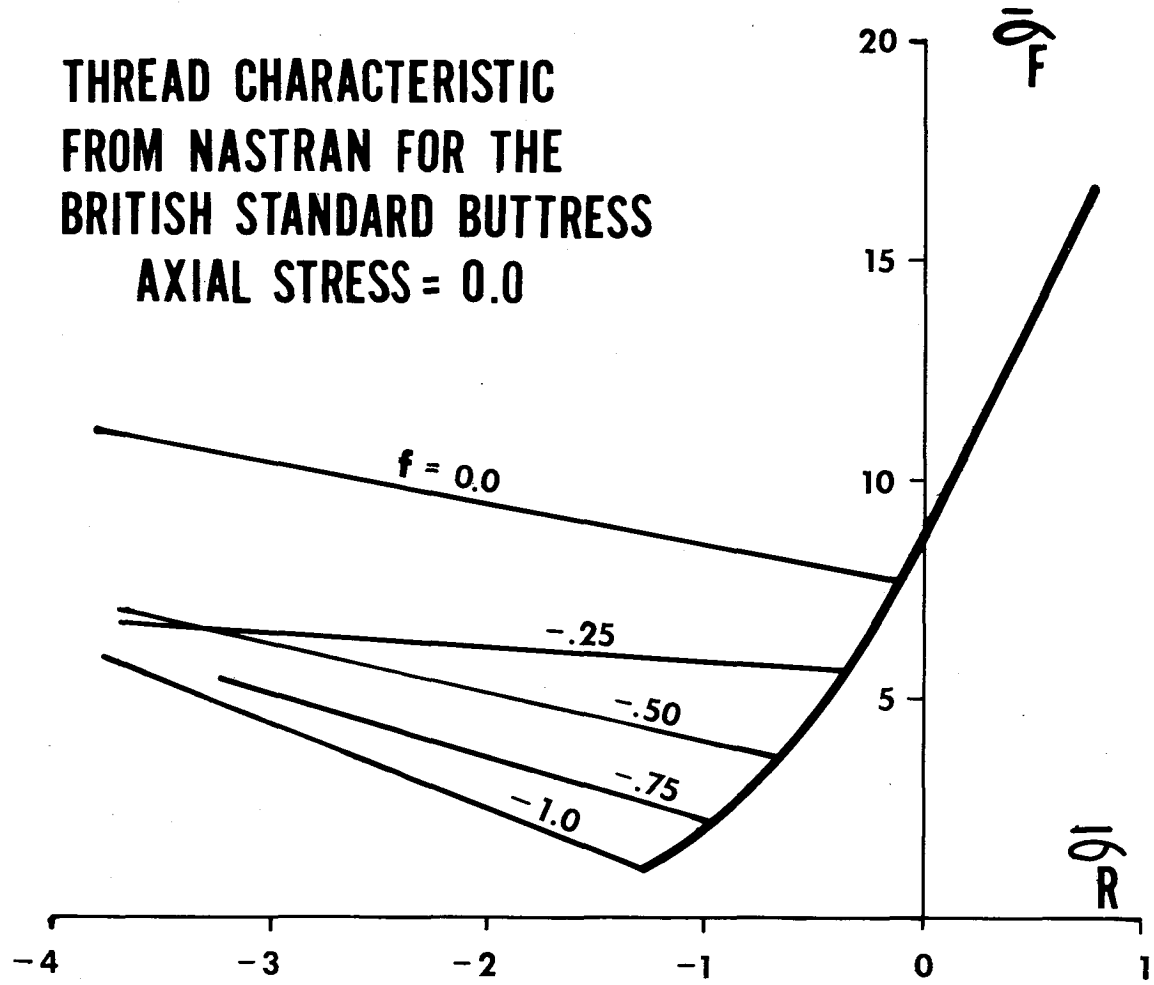


Figure 5.

THREAD CHARACTERISTIC
FROM NASTRAN FOR THE
BRITISH STANDARD BUTTRESS

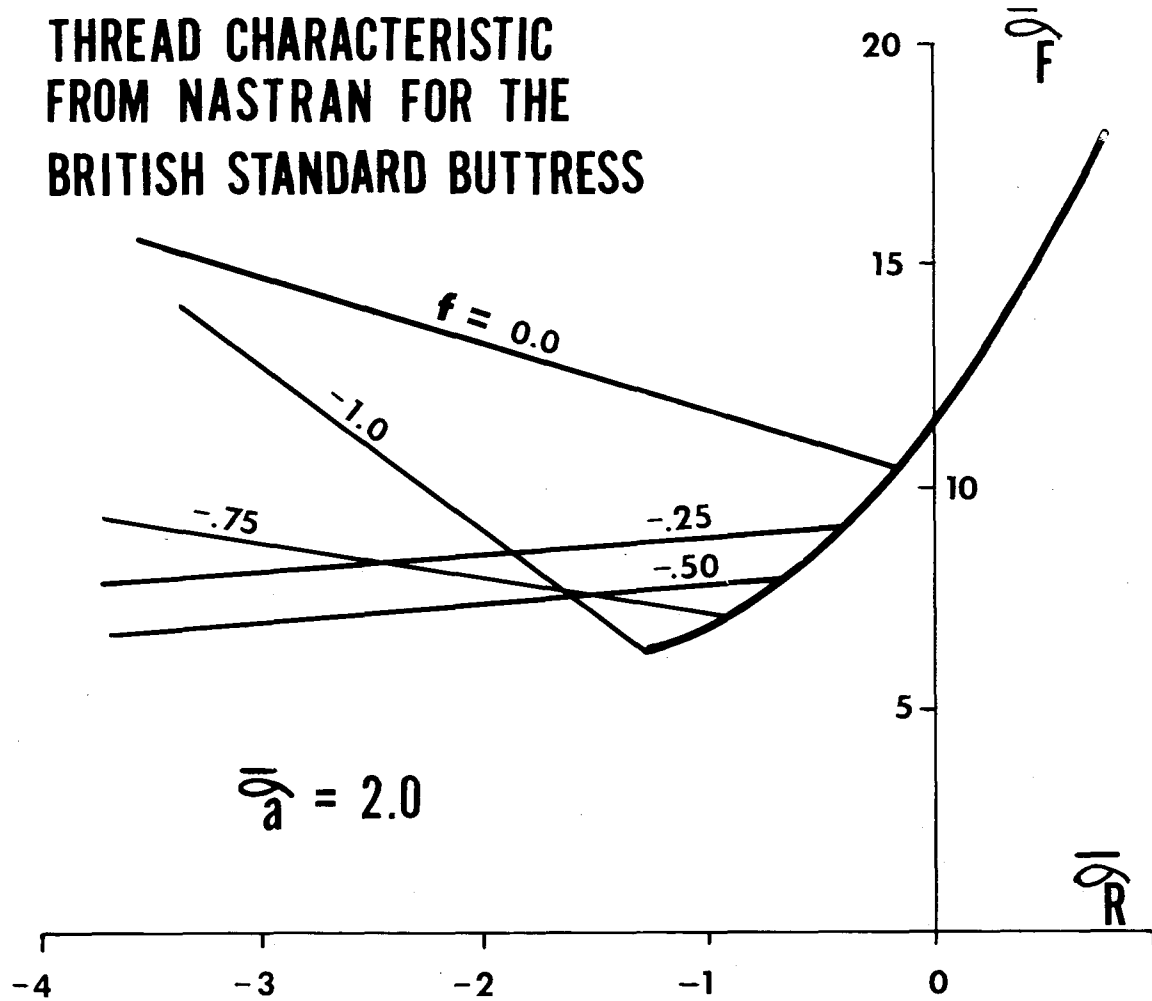


Figure 6.